ceedings of 7th International Symposium on Power Semiconductor Devices, p. 279, Yokohama (1995).
10. S. Bengtsson, *J. Electron. Mater.*, **21**, 841 (1992).
11. C. Harendt, B. Hoffinger, H.-G. Graf, and E. Penteker, *Sens. Actuators A*, **25-27**, 87 (1991).
12. W .Kern and D. A. Puotinen, *RCA Rev.*, **31**, 187 (1970).
13. M. J. J. Theunissen, A. H. Goemans, A. J. R. de Kock, J. Haisma, C. W. T. Bulle-Lieuwma, and D. E. W. Vandenhoudt, *This Journal*, **137**, 3975 (1990).
14. Q.-Y. Tong, H.-Z. Zhang, and M. Quing, *Electron.Lett.*, **27**, 288 (1991).
15. W. D. Kingery, *Introduction to Ceramics*, Chap. 4, 5, 14, John Wiley & Sons, Inc., New York (1970).
16. T. Abe, T. Takei, A. Uchiyama, K. Yoshizawa, and Y. Nakazato, *Jpn. J. Appl. Phys.*, **29**, L2311 (1990).
17. A. Yamada, B.-L. Jiang, G. A. Rozgony, H. Shirotori, O. Okabayashi, and M. Kawashima, *This Journal*, **138**, 2486 (1991).
18. V. B. Voronkov, I. V. Grekhov, and V. A. Kozlov, *Phys. Tech. Semicond.*, **25**(2), p. 208 (1991).

Effects of Bromine-Methanol and Hydrogen Chloride Pretreatments on Pt/Al/n-InP Diodes

Wen Chang Huang, Tan Fu Lei, and Chung Len Lee

Department of Electrical Engineering and Institute of Electronics, National Chiao Tung University, Hsinchu, Taiwan

ABSTRACT

This paper reports the passivation effects of bromine-methanol (Br/M) and hydrogen chloride (HCl) treatments on the n-InP surface to form Pt/Al/n-InP diodes. It was found that Br/M and HCl passivated the n-InP surface. The Br/M-dipped and the HCl-dipped Pt/Al/n-InP diodes exhibited a barrier height of 0.83 and 0.86 eV, respectively, and a low reverse leakage current of 7.07×10^{-7} and 1.10×10^{-7} A/cm^2 at -3 V, respectively. The secondary ion mass spectroscopy and electron spectroscopy for chemical analysis showed that the Br/M or HCl treatment made formation of bromides and chlorides on the n-InP surface, respectively. They also revealed the existence of Al_2O_3, which is believed to be formed with the native In_2O_3 during the Al evaporation. This, which made the diodes be of the metal-insulator-semiconductor structure, in conjunction with the passivation effect of bromides and chlorides, improved the diode characteristics and produced the high barrier heights.

Introduction

Indium phosphide is an attractive III-V compound semiconductor for high speed metal semiconductor field effect transistors (MESFETs)[1] due to its high electron mobility and high radiation hardness. For these InP devices, metal-semiconductor (MS) contacts and/or metal-insulator-semiconductor (MIS) tunnel junctions are imperative. The surface Fermi level pinning, arising from the large surface state density and other nonstoichiometric defects, makes it very difficult to achieve a Schottky barrier height greater than 0.5 eV for n-InP.[2-4] Such a small barrier causes a large reverse leakage current and degrades the performance of the devices. Many techniques have been proposed to increase the barrier height for the metal/n-InP Schottky diode. For example, a thin interfacial oxide layer between the contacting metal(s) and the n-InP substrate was incorporated increasing the barrier height.[5-11] Techniques such as depositing the metal at a low temperature (77 K) to form the metal/n-InP contact to obtain a high Schottky barrier height,[12] and use of composite metals to form the Schottky contact have been reported. For the latter, Dunn *et al.*[13] reported a barrier height up to 0.65 eV by using the Ag/Al contact to n-InP and Huang *et al.*[14] reported a barrier height at 0.74 eV by using Pt/Al to form a contact to n-InP.

In fabricating InP devices, bromine in methanol (Br/M) is often used for InP to prepare a clean surface. This bromine-based etchant yields a 2 to 20 Å film which contains oxidized phosphorus in the form of $InPO_4$, $In(PO_3)_3$, or H_3PO_4 [15-17] on the surface of InP. In addition, HCl is also often used to treat the InP surface. HCl has been found to leave a thinner film, which is composed of indium-rich oxides such as In_2O_3 and $In(OH)_3$, [15,17] on the InP surface. Since the barrier height of a Schottky diode is very sensitive to its surface condition, it is expected that different surface treatments by different etching solutions will result in different barrier heights. In this paper, we report a detailed study of the Pt/Al/n-InP diode after its treatment by Br/M on its InP surface before metallization. Electron spectroscopy for chemical analysis (ESCA) and secondary ion mass spectroscopy (SIMS) are used to investigate its surface and the results are used to correlate with the electrical characteristics of the diode. It is shown that the Br/M-pretreated diode can exhibit an effective barrier height of 0.83 eV and a reverse leakage current of 7.07×10^{-7} A/cm^2 at -3 V, and the HCl-pretreated diode can have an effective barrier height up to 0.86 eV and a reverse leakage current density as low as 1.11×10^{-7} A/cm^2 at -3 V.

Diode Fabrication and Measurement

The diodes used in this study were made on a (100) InP substrate with a carrier concentration of 5 to 9×10^{15} cm^{-3}. Low resistance ohmic contact on the back side was formed by evaporating an AuGeNi eutectic source (84% Au, 12% Ge, 4% Ni by weight), followed by annealing at 400°C for 3 min. During the annealing process, InP proximity cap was placed on the front surface of the substrate to prevent phosphorus out-diffusion. The wafers were then degreased with acetone (ACE), methanol, and deionized water in sequence then soaked in H_2SO_4 (98%) for 3 min and etched in NH_4OH:H_2O_2:H_2O = 3:1:15 for 3 min to remove surface damage. A thickness on 2000 Å SiO_2 was then deposited on the front side of wafers, and the contact pattern was defined photolithographically. The SiO_2 in the contact windows was removed in buffered oxide etching (BOE), and the wafers were then rinsed in deionized water. Samples of Br/M-pretreated diodes and HCl-pretreated diodes were prepared, and their characteristics were compared with the control diodes. For control diodes, Pt (500 Å) and Al (85 Å) were deposited sequentially to form the multilayer electrode for the devices after the contact window was removed. For the Br/M-pretreated diodes, samples were separated into two groups for two cleaning processes: one group was dipped in 5% bromine-methanol (Br/M) for 10 s and N_2 dried and then metallized (called Br/M-dipped diodes); the other group was dipped in 5% bromine-methanol for 10 s, rinsed in DI water and N_2 dried and then metallized (called Br/M cleaned-diodes). Similar processes were also performed on the HCl-pretreated diodes, *i.e.*, the HCl-dipped diodes were dipped in an HCl:H_2O = 1:1 etchant for 10 s and N_2 dried and then

Downloaded on 2014-04-28 to IP 140.113.38.11 address. Redistribution subject to ECS terms of use (see ecsdl.org/site/terms_use) unless CC License in place (see abstract).

metallized, the HCl-cleaned diodes were dipped in the $HCl:H_2O$ = 1:1 for 10 s, rinsed in DI water, N_2 dried, and then metallized. For metallization, metals Pt (1000 Å) and Pt (500 Å)/Al (85 Å) were deposited on each pretreated diode, respectively, at a vacuum of 7×10^{-7} Torr, and metal patterns were obtained by using a lift-off process. There were four different areas for each type of diodes, *i.e.*, 1.12×10^{-3}, 4.6×10^{-4}, 2.25×10^{-4}, and 6.12×10^{-5} cm^2.

ESCA (Al K_α radiation with 1486.8 eV photon energy) was used to estimate the composition of the pretreated InP surfaces. For these analyses, the InP wafer and Al/InP wafers were specially prepared with the same cleaning processes applied to the control diode, the Br/M-dipped diode, and the HCl-dipped diode. SIMS, of which the primary beam was a $^{133}Cs^+$ beam at 10 keV with a current of 16 nA and a rastering area of 0.225 × 0.225 cm, was used to analyze the distribution of all elements of the deposited films. The current-voltage (*I-V*) characteristics was measured by an HP4145B. The capacitance-voltage (*C-V*) characteristics were measured by a Keithley 590 C-V analyzer.

Results and Discussion

Electrical characteristics of Pt/Al/n-InP diodes.—The effective barrier heights, $\varnothing_b$, were derived for comparison with other works. Figure 1 shows the *I-V* characteristics of the Br/M-dipped, Br/M-cleaned, and control Pt/Al/n-InP diodes, respectively. For the Br/M-dipped Pt/Al/n-InP diode, it exhibits a forward characteristic with an ideality factor of n = 1.14 over five decades. The effective barrier height $\varnothing_b$ derived is 0.83 eV. It also shows a low saturation current density of 1.09×10^{-8} A/cm^2. The leakage current is 7.07×10^{-7} A/cm^2 at −3 V. For the Br/M-cleaned diode and control diode, their effective barrier heights $\varnothing_b$ are 0.70 and 0.73 eV, and their ideality factors are 1.35 and 1.20, respectively. The reverse leakage current densities at −3 V are 4.06×10^{-5} and 1.34×10^{-5} A/cm^2, respectively. Although the control diode and the Br/M-cleaned diode have good *I-V* characteristics as compared to conventional metal/n-InP diodes, the Br/M-dipped diode has the best forward and reverse characteristics. The effective barrier height of the diode is higher than that of control diode by about 0.1 eV, and is higher than that of the conventional metal/n-InP Schottky diode by about 0.3 to 0.4 eV.[2-4] The reverse leakage current is smaller than that of the control diode by more than two orders of magnitude. For the Br/M-cleaned diode, the electrical characteristics do not have too much difference from that of the control diode.

Figure 2 shows the C^{-2}-V characteristics of the corresponding diodes of Fig. 1. The three curves have slight differences on their slopes which imply there are slight differences on their effective surface carrier concentrations. The effective surface concentrations are derived to be 3.13 × 10^{15}, 4.87 × 10^{15}, and 4.11 × 10^{15} cm^{-3} for the Br/M-dipped diode, the Br/M-cleaned diode, and the control diode, respectively. From the intercept on the voltage axis V_i, the barrier height can be determined[2] to be $\varnothing_{cb} = V_i + V_n + kT/q$, where V_n is the energy difference of the Fermi level from the minimum of the conduction band. From these plots, the barrier height $\varnothing_{cb}$ was found to be 0.96 eV for the Br/M-dipped diode, 0.68 eV for the Br/M-cleaned diode, and 0.83 eV for the control sample diode, respectively. The barrier height derived by the *C-V* measurement generally is higher than that derived by the *I-V* measurement due to the existence of an interfacial layer between the metal and the semiconductor.[2] For the Br/M-cleaned diode, the value of the barrier height derived from the *C-V* curve is less than that derived from the *I-V* curve. This may imply that the interfacial layer between the metal and the InP substrate produced by Br/M dipping have been washed out during the DI water rinsing. And this changed the surface states of InP and caused the barrier height obtained for this diode to be less than that of the control diode.

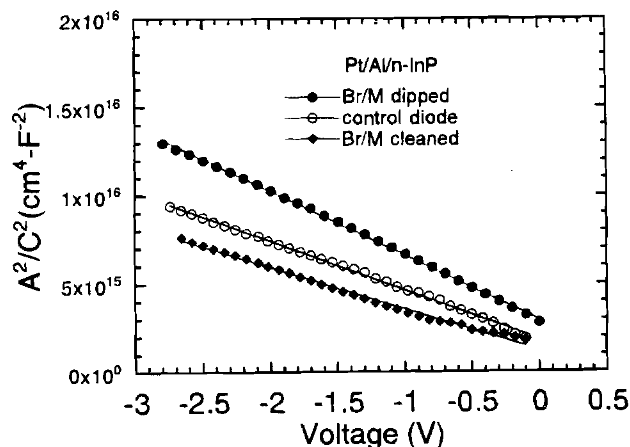

Fig. 2. The C^2-V characteristics of the control diode, Br/M-dipped, and Br/M-cleaned Pt/Al/n-InP diodes.

The *I-V* characteristics of the HCl-pretreated diodes are shown in Fig. 3. Similar to the electrical characteristics of the Br/M-pretreated diode, the HCl-dipped diode gives better electrical characteristics than that of the HCl-cleaned diode and the control diode. A rather high effective barrier of 0.86 eV was obtained for the HCl dipped diode, and it is higher by about 0.13 eV than that of the control diode, which is 0.73 eV. The barrier height of the HCl-cleaned diode, which is 0.70 eV, is a little lower than

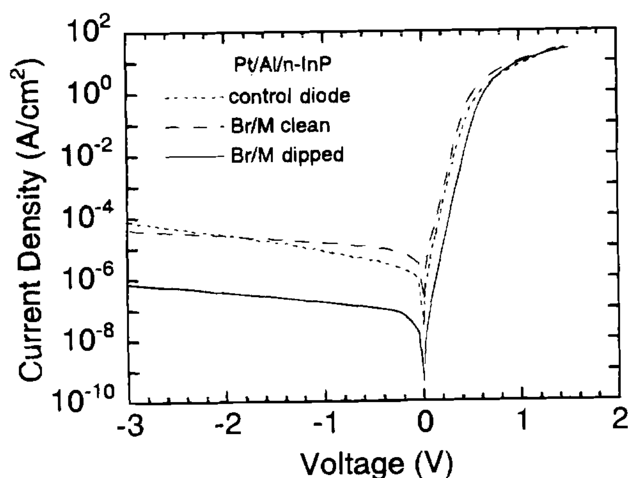

Fig. 1. The *I-V* characteristics of the control diode, Br/M-dipped, and Br/M-cleaned Pt/Al/n-InP diodes.

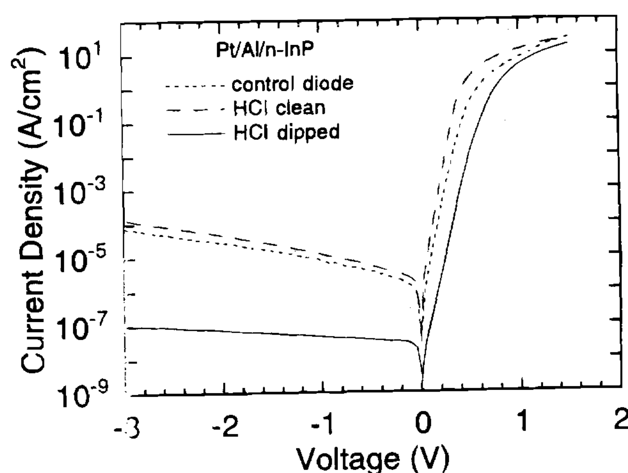

Fig. 3. The *I-V* characteristics of the control diode, HCl-dipped, and HCl-cleaned Pt/Al/n-InP diodes.

Downloaded on 2014-04-28 to IP 140.113.38.11 address. Redistribution subject to ECS terms of use (see ecsdl.org/site/terms_use) unless CC License in place (see abstract).

Table I. Summary of *I-V* characteristics of the Pt/Al/n-InP diodes with different surface pretreatments.

	Pt/Al/n-InP			
Preparation	Ideality factor	J_o (A/cm^2)	$\varnothing_b$ (eV)	J_r (A/cm^2) at −3 V
Control diode	1.20	4.38E−7	0.73	1.34E−4
Br/M-cleaned	1.35	1.76E−6	0.70	4.06E−5
Br/M-dipped	1.14	1.09E−8	0.83	7.07E−7
HCl-cleaned	1.11	1.50E−6	0.70	4.11E−4
HCl-dipped	1.30	3.61E−9	0.86	1.11E−7

that of the control diode. The ideality factor of the HCl-dipped diode is 1.3, and the saturation current density is 3.6×10^{-9} A/cm^2. The reverse leakage current is 1.11×10^{-7} A/cm^2 at −3 V, approximately three orders of magnitude lower than that of the control diode. The ideality factor and the reverse leakage are 1.1 and 4.11×10^{-4} A/cm^2, respectively, for the HCl-cleaned diode. The parameters of all these Pt/Al/n-InP diodes are summarized on Table I. The *C-V* characteristics of the same HCl-pretreated diode are shown in Fig. 4. The built-in potential of the HCl-dipped diode, the HCl-cleaned diode, and the control diode are 0.84, 0.53, and 0.68 eV, respectively. The effective surface carrier concentrations derived from these curves are 3.25×10^{15}, 4.00×10^{15}, and 4.11×10^{15} cm^{-3}, respectively, and the barrier heights, $\varnothing_{cb}$, are 0.99, 0.68, and 0.83 eV, respectively. It is also noted that the $\varnothing_{cb}$ values of the HCl-dipped diode and the control diode are larger than those derived from *I-V* characteristics, respectively, but for the HCl-cleaned diode, the *C-V* value is less than the *I-V* value. The same reason stated above for the Br/M-cleaned diode may be used to explain this, *i.e.* the interfacial layer produced by HCl-dipping had been washed away by the after DI water rinsing. This can also be supported by the fact that the barrier height obtained from the *I-V* characteristics for this diode is the lowest among the three diodes.

The SIMS analysis results.—Figure 5a, b, and c show the SIMS in-depth profiles of element distributions for the Pt/Al/n-InP control diode, the Br/M-dipped diode, and the HCl-dipped diode, respectively. In Fig. 5a, an oxygen peak is observed at the interface of the metals and the InP substrate. This is believed to be due to the aluminum oxide which was formed during the Al evaporation.[13,14] Because of this aluminum oxide, which gave the Pt/Al/n-InP device a metal-insulator-semiconductor (MIS) structure, resulting in a higher effective barrier height, 0.73 eV, than that of the conventional metal/n-InP diodes. In Fig. 5b, which is SIMS profiles of Br/M-dipped diode, bromine is observed at the contact interface. Also, oxygen, which had a broader distribution than that of the control diode of Fig. 5a and nearly overlayed with bromine and aluminum, is observed. This suggests that the higher barrier height of the Br/M-dipped Pt/Al/n-InP was also caused by the existence of aluminum oxide at the contact interface and the existence of bromine further increased the barrier height. As it is to be shown later in the ESCA analysis, the bromine reacted with aluminum and indium to form Al-Br and In-Br bonds which passivated the InP surface. This same phenomenon is also observed in the profiles of the

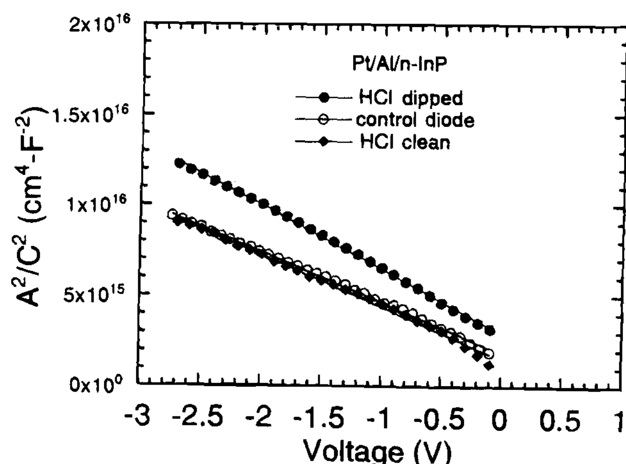

Fig. 4. The C^2-*V* characteristics of the control diode, HCl-dipped, and HCl-cleaned Pt/Al/n-InP diodes.

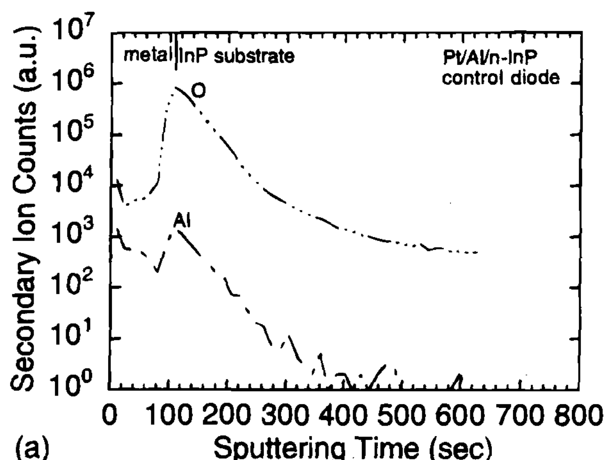

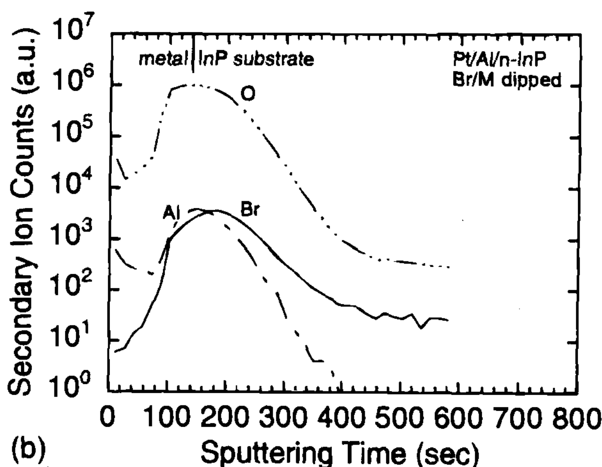

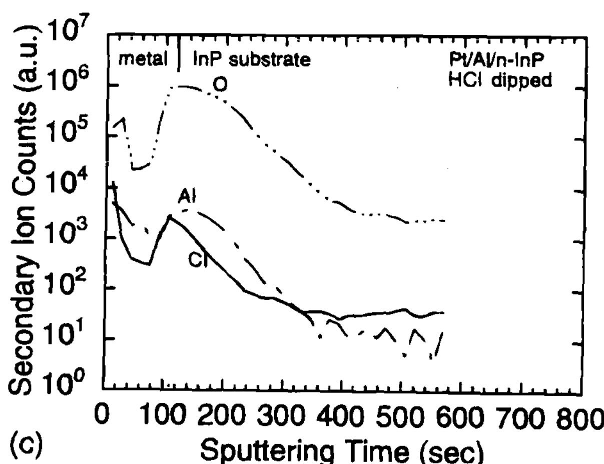

Fig. 5. The SIMS in-depth profiles of element distributions of (a) the control diode, (b) the Br/M-dipped Pt/Al/n-InP diode, and (c) the HCl-dipped Pt/Al/n-InP diode, respectively.

Downloaded on 2014-04-28 to IP 140.113.38.11 address. Redistribution subject to ECS terms of use (see ecsdl.org/site/terms_use) unless CC License in place (see abstract).

HCl-dipped Pt/Al/n-InP diode of Fig. 5c. In those profiles, oxygen and chlorine are also observed at the contact interface of the Pt/Al/n-InP diode. It is also believed that this is the reason which made the diode have the high barrier height of 0.86 eV.

The ECSA analysis results.—The surface compositions of the Al/InP wafers with the control diode, the Br/M-dipped diode, and the HCl-dipped diode cleaning steps, respectively, were analyzed by ESCA. For comparison, InP wafers prepared with similar procedures with the control, the Br/M-dipped, and HCl-dipped steps, respectively, but without devices made on them were also analyzed by ESCA. The results are shown in Fig. 6, 7, 8, 9, 10, and 11. The spectra for the C_{1s}, P_{2p}, O_{1s}, and Al_{2p} peaks were recorded at take-off angles of 54° to 90° to the sample surface. Due to the charging effect of samples, the binding energy of 285 eV of the peak of C_{1s}, which was attributed to the CH-type residue in the hydrocarbon environment, was chosen for correction.[15]

Figure 6a, b, and c, show the results of InP control wafer which was only subjected to the standard cleaning procedure without the Br/M or HCl dipping. In Fig. 6a, the peak centered at the binding energy of 128.8 eV corresponds to the P_{2p} signal of the InP substrate. The binding energy of 133.5 eV of P_{2p} signal,[15] which corresponds to the binding energy of phosphorus in $InPO_4$, is not observed at the spectrum. In Fig. 6b, the peak at 444.4 eV is close to the peak

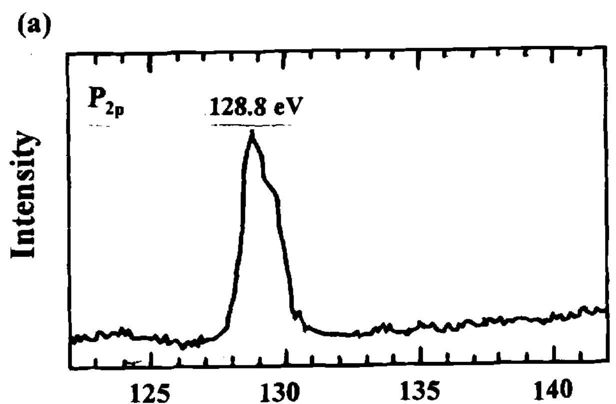

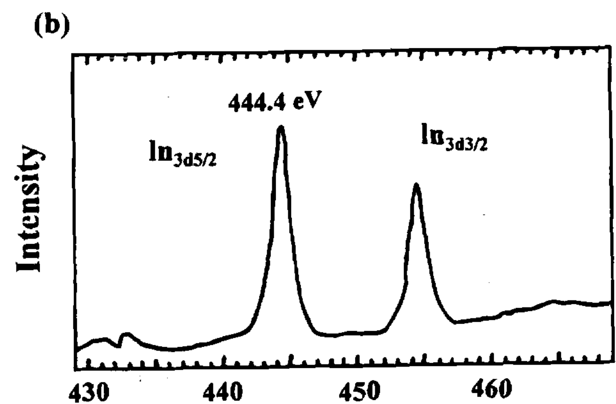

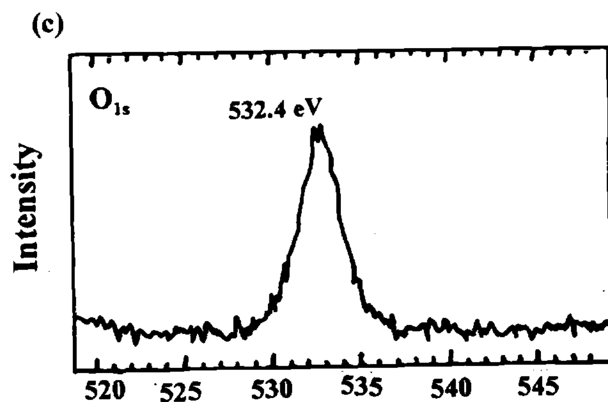

Binding Energy (eV)

Fig. 6. The ESCA spectra of the standard clean InP surface: (a) the P_{2p} spectrum, (b) the In_{3d} spectrum, and (c) the O_{1s} spectrum.

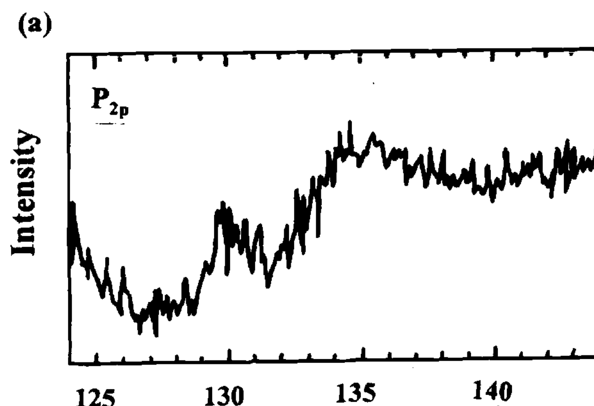

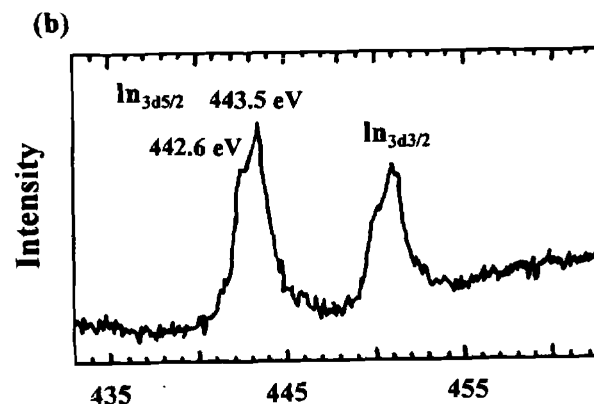

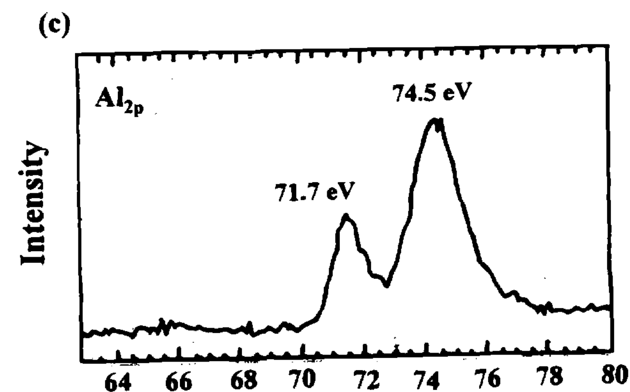

Binding Energy (eV)

Fig. 7. The ESCA spectra of the standard clean Al/InP surface: (a) the P_{2p} spectrum, (b) the In_{3d} spectrum, and (c) the Al_{2p} spectrum.

Downloaded on 2014-04-28 to IP 140.113.38.11 address. Redistribution subject to ECS terms of use (see ecsdl.org/site/terms_use) unless CC License in place (see abstract).

signal of $In_{3d5/2}$ of the InP substrate (444.3 ± 0.1 eV) or In_2O_3 (444.8 ± 0.2 eV),[15,18] so the In_{3d} signal may come from the InP substrate or the In_2O_3, which was formed during the processing steps. Also, in this spectrum, the peak of 445.7 eV, which corresponds to the peak of $In_{3d5/2}$ of $InPO_4$, is not observed. Hence, it can be concluded that $InPO_4$ did not exist at the interface. In Fig. 6c, the O_{1s} spectrum has a peak at 532.4 eV with a full width at half maximum (FWHM) of 3 eV. The binding energy of O_{1s} of In_2O_3 is 530.5 eV.[19] This, in conjunction with the above finding at Fig. 6a and b, suggests that In_2O_3, not P-O related compound, existed at the contact interface.

Figures 7a, b, and c are the results for the Al/InP control wafer which only went through the standard cleaning procedure. In Fig. 7a, no obvious phosphorus peak in the P_{2p} spectrum is observed. In Fig. 7b of the $In_{3d5/2}$ spectrum, the 444.4 eV peak (as shown in Fig. 6b) disappears and a new peak of 443.5 eV for $In_{3d5/2}$ appears. The 443.5 eV peak corresponds to $In_{3d5/2}$ of metallic indium.[19] In Fig. 7c of the Al_{2p} spectrum, two peaks are observed. The peak of 71.7 eV corresponds to metallic aluminum and the peak at 74.5 eV comes from Al_2O_3.[19,20] Hence, combining the above results (Fig. 6 and 7) with the SIMS data of Fig. 5a, we can deduce for this Al/InP contact for the following: initially, there was native oxide, In_2O_3, existing at the InP surface after it went through the cleaning process. During the aluminum deposition, aluminum formed aluminum oxide with oxygen from the dissolved In_2O_3, in addition to the residual oxygen in the environment. At the same time, InP also decomposed and In out-diffused to the surface of the Al overlayer.

Figure 8a and b shows the ESCA In_{3d} and P_{2p} spectra for the Br/M-dipped InP substrate, respectively. In Fig. 8a, the main $In_{3d5/2}$ peak centered at 445.0 eV corresponds to the In peak of In_2O_3. A shoulder of the binding energy at 446.0 eV on this main peak is also observed. This binding energy might result from two possible phases, $InPO_4$ and $InBr_3$.[20] For the P_{2p} spectrum of Fig. 8b, the peak at 129.5 eV was from the InP substrate since the P_{2p} binding energy of $InPO_4$ is 133.5 eV. Hence, it may be concluded that on this Br/M-dipped InP surface there was In_2O_3 and/or $InBr_3$.

Figure 9a, b, and c shows the ESCA $In_{3d5/2}$, P_{2p}, and Al_{2p}, and Br_{3d} spectra for the Br/M-dipped Al/InP wafer, respectively. In Fig. 9a, there are two peaks, one centered at 445 eV and the other centered at 446.1 eV. The former peak corresponds to the signal of In_2O_3, and the latter corresponds to $InBr_3$.[20] For the P_{2p} spectrum in Fig. 9b, the

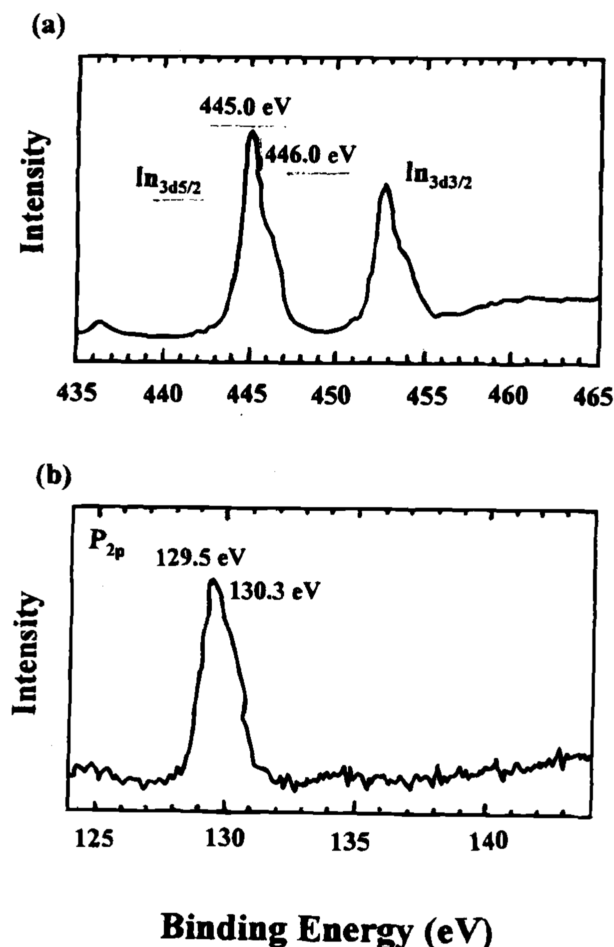

Fig. 8. The ESCA spectra of the Br/M-dipped InP surface: (a) the In_{3d} spectrum, (b) the P_{2p} spectrum.

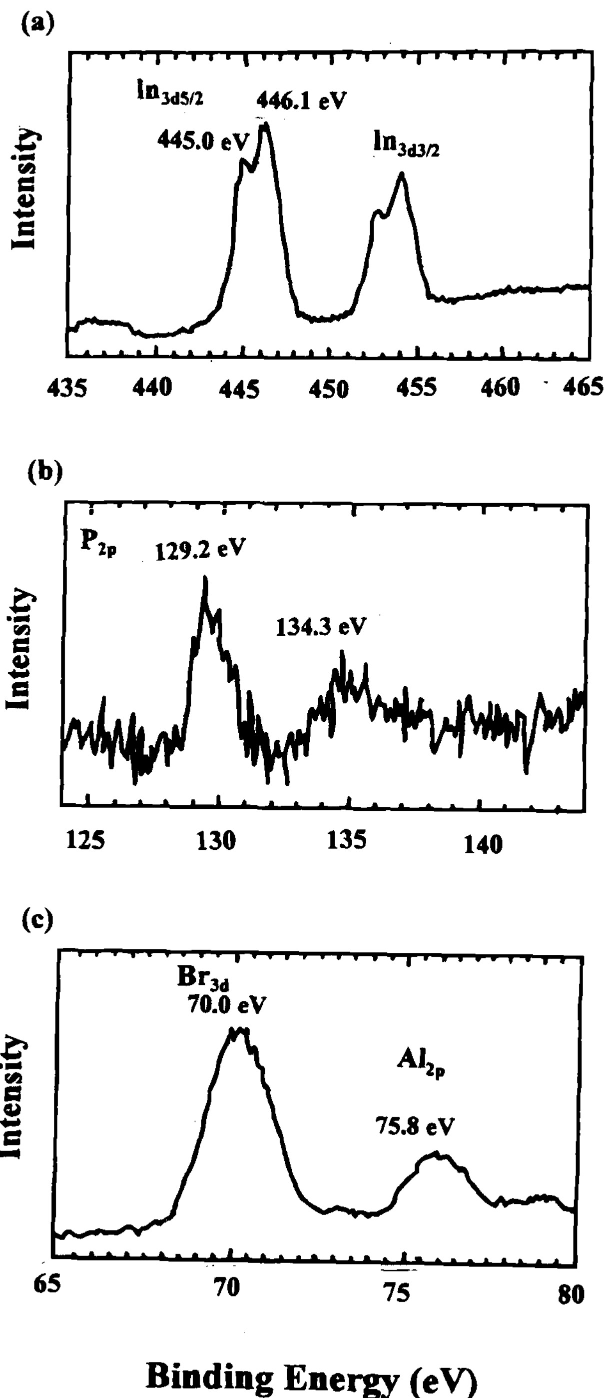

Fig. 9. The ESCA spectra of the Br/M-dipped Al/InP surface: (a) the In_{3d} spectrum, (b) the P_{2p} spectrum, and (c) the Al_{2p} and Br_{3d} spectrum.

Downloaded on 2014-04-28 to IP 140.113.38.11 address. Redistribution subject to ECS terms of use (see ecsdl.org/site/terms_use) unless CC License in place (see abstract).

peaks of 129.2 and 134.3 eV correspond to the P of the InP substrate and the $InPO_4$ on the InP surface, respectively. In Fig. 9c, the peak signal of Al_{2p} is centered at 75.8 eV which is higher than that of Al_2O_3, which is 74 to 74.6 eV. Hence, it possibly came from the Al-Br bond.[21] Compared to the results of Fig. 7, which is for the Al/InP sample of the standard cleaning process, the Br/M-dipped Al/InP sample shows more complete reaction between Al and InP substrate, and does not show any metallic Al (binding energy 72.5 eV) left. Also, the indium spectrum, for which no metallic indium was found, is different from that of the standard cleaning Al/InP sample. Hence, it can be deduced that the surface compositions of the Br/M-dipped Al/InP sample are In_2O_3, $InBr_3$, and Al-Br bond.

For the HCl-dipped InP surface, Fig. 10a shows the $In_{3d5/2}$ signal which had a peak at 444.9 eV with a shoulder at 446.0 eV. The former binding energy corresponds to In_2O_3 and the latter corresponds to $InCl_3$, respectively.[21] Figure 10b shows the binding energy of P_{2p} centered at 129.2 eV, which came from the InP substrate. No phosphorus-related oxide, whose binding energy is around 133.5 eV, is observed. In Fig. 10c, the Cl_{2p} spectrum shows a combination of energy peaks of 199.4 and 200.9 eV. The former binding energy corresponds to $InCl_3$ and the latter corresponds to the compounds of chlorine, carbon, or hydrogen.[20]

For the HCl-dipped Al/InP surface, Fig. 11a shows the $In_{3d5/2}$ spectrum with the peaks at 443.1 and 445.6 eV, which correspond to metallic indium and $InCl_3$, respectively. In addition, there is a weak signal, which results from In_2O_3 (444.7 eV), observed. For the Al_{2p} spectrum as shown in Fig. 11b, the peak at 72 eV is related to metallic

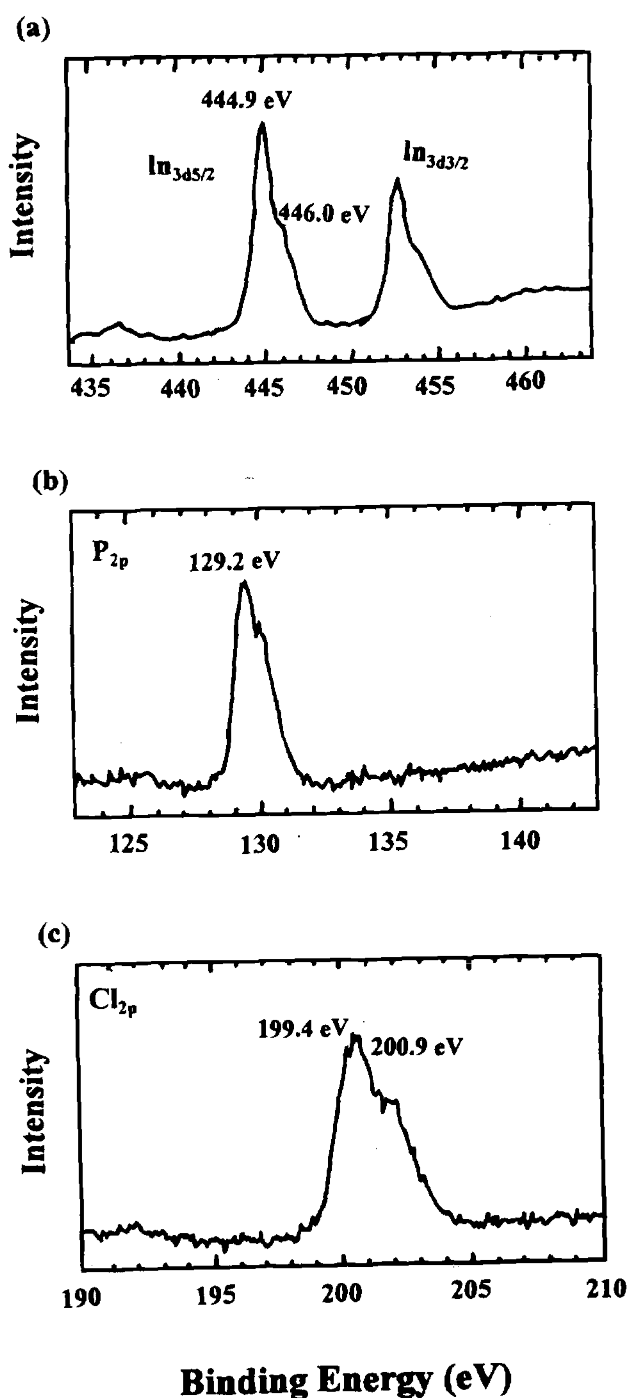

Fig. 10. The ESCA spectra of the HCl-dipped InP surface: (a) the In_{3d} spectrum, (b) the P_{2p} spectrum, and (c) the Cl_{2p} spectrum.

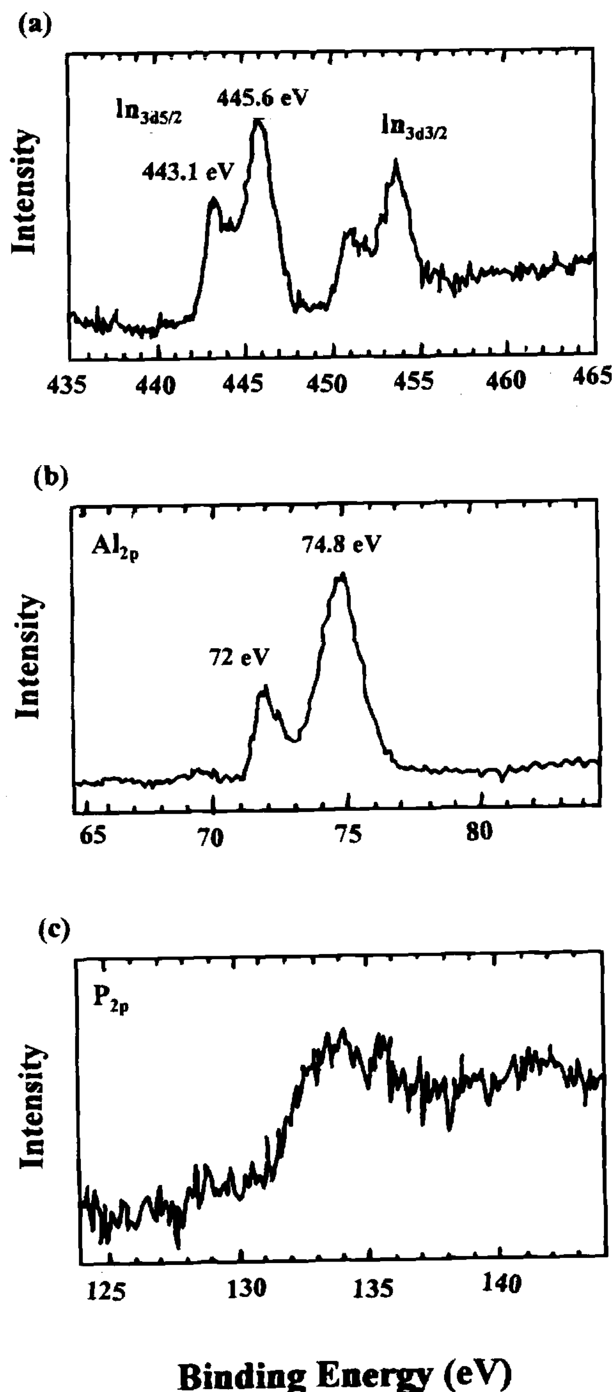

Fig. 11. The ESCA spectra of the HCl-dipped Al/InP surface: (a) the In_{3d} spectrum, (b) the Al_{2p} spectrum, and (c) the P_{2p} spectrum.

Downloaded on 2014-04-28 to IP 140.113.38.11 address. Redistribution subject to ECS terms of use (see ecsdl.org/site/terms_use) unless CC License in place (see abstract).

aluminum,[22] and the peak at 74.8 eV is related to Al_2O_3 or $AlCl_3$.[20] Figure 11c shows the P_{2p} spectrum and there is no phosphorus-related compound observed. It is believed that for this HCl-dipped Al/InP surface, aluminum reacted with In_2O_3 and the InP substrate to form Al_2O_3 and $AlCl_3$ during the aluminum deposition and some metallic indium floated to the surface.

The above results can be summarized as follows: InP, after it went through the standard cleaning process, In_2O_3 was formed at the surface. This In_2O_3 decomposed during the following Al evaporation and Al reacted with the decomposing oxygen, as well as the residual oxygen in the environment, to form Al_2O_3. For the InP wafer applied with Br/M or HCl dippings, $InBr_3$ or $InCl_3$ formed, respectively. When these Br/M or HCl-dipped InP wafers were evaporated with Al for contacts, in addition to Al_2O_3, Al-Br or Al-Cl compounds also formed during the evaporation, respectively. Also, some of In_2O_3 also existed. It is believed that it was the formed Al_2O_3, as well as the residual In_2O_3, acted as the insulator for this Al/InP to become a MIS structure to achieve a high barrier height. The Br/M or the HCl dipping provided Br or Cl to form $InBr_3$ or $InCl_3$ at the surface to passivate the interface. This further enhanced the barrier height.

Conclusions

This paper reports the passivation effects of bromine-methanol (Br/M) and hydrogen-chloride (HCl) treatments on the Pt/Al/n-InP diode. It was found that Br/M or HCl pretreatment of the n-InP surface gave the diodes formed on the treated n-InP good electrical characteristics. The Pt/Al/n-InP diode formed by Br/M dipping exhibited a barrier height of 0.83 eV and a low reverse leakage current of 7.07×10^{-7} A/cm^2 at -3 V and the diode formed by HCl dipping showed a barrier height of 0.86 eV, and a reverse leakage current of 1.10×10^{-7} A/cm^2 at -3 V. SIMS and ESCA analyses showed that In_2O_3 existed on the InP surface after the InP wafer went through the standard cleaning process, this In_2O_3 decomposed during the following Al evaporation to form Al_2O_3, and the Br/M or HCl treatments on the n-InP surface caused formation of interfacial layers of bromides and chlorides, respectively. It is believed that the aluminum-oxide thus formed, acts as a tunneling insulator to make the diodes be metal-insulator-semiconductor diodes and the bromides or chlorides formed passivate the interface of the diodes. These made the diodes have high barrier heights and good electrical characteristics.

Acknowledgment

This work was supported by the National Science Council of the Republic of China through Contract No. NSC-84-2215-E009-023.

Manuscript submitted Jan. 22, 1996; revised manuscript received Nov. 4, 1996.

REFERENCES

1. J. S. Barrera and R. J. Archer, *IEEE Trans. Electron Devices,* **ED-22**, 1023, (1975).
2. E. H. Rhoderick and R. H. Williams, in *Metal-Semiconductor Contacts,* 2nd ed., Clarendon, Oxford (1988).
3. E. Hokelek and G. Y. Robison, *Solid-State Electron.,* **24,** 99 (1981).
4. L. J. Brillson and C. F. Brucker, *J. Vac. Sci. Technol.,* **21,** 564 (1982).
5. T. Sugino, H. Yamamoto, Y. Sakamoto, H. Ninomiya, and J. Shirafuji, *Jpn. J. Appl. Phys.,* **30**, L1439 (1991).
6. Y. H. Jeong, G. T. Kim, S. T. Kim, K. I. Kim, and W. J. Chung, *J. Appl. Phys.,* **69,** 6699 (1991).
7. D. T. Quan and H. Hbib, *Solid-State Electron.,* **36**, 339 (1993).
8. H. Yamagishi, *Jpn. J. Appl. Phys.,* **25,** 1691 (1986)
9. K. Kamimura, T. Suzuki, and A. Kunioka, *J. Appl. Phys.,* **51,** 4905 (1980).
10. O. Wada, A. Majerfeld, and P. N. Robson, *Solid-State Electron.,* **25,** 381 (1982).
11. Y. S. Lee and W. A. Anderson, *J. Appl. Phys.,* **65,** 4051 (1989).
12. Z. Q. Shi, R. L. Wallace, and W. A. Anderson, *Appl. Phys. Lett.,* **59,** 446 (1991).
13. J. Dunn and G. B. Stringfellow, *J. Electron. Mater.,* **17,** 181 (1988).
14. W. C. Huang, T. F. Lei, and C. L. Lee, *J. Appl. Phys.,* **78,** 291 (1995).
15. D. T. Clark, T. Fok, G. G. Robert, and R. W. Sykes, *Thin Solid Films,* **70,** 261 (1980).
16. A. Guivarc'h, H. L'Haridon, G. Pelous, G. Hollinger, and P. Pertosa, *J. Appl. Phys.,* **55,** 1139 (1984).
17. P. A. Bertrand, *J. Vac. Sci. Technol.,* **18,** 28 (1981).
18. P. R. Segar, C. A. Koval, B. E. Koel, and S. C. Gebhard, *This Journal,* **137,** 544 (1990).
19. J. R. Waldrop, S. P. Kowalczyk, and R. W. Grant, *Appl. Phys. Lett.,* **42,** 454 (1983).
20. C. D. Wager, *Handbook of X-Ray and Ultraviolet Photoelectron Spectroscopy,* Briggs, Editor, Heyden and Sons, London (1977).
21. B. H. Freeland, J. J. Habeeb, and D. G. Tuck, *Can. J. Chem.,* **55,** 1528 (1977).
22. T. Kendelewicz, W. G. Petro, J. A. Silberman, I. Lindau, and W. E. Spicer, *J. Vac. Sci. Technol.,* **B1,** 623 (1983).

Downloaded on 2014-04-28 to IP 140.113.38.11 address. Redistribution subject to ECS terms of use (see ecsdl.org/site/terms_use) unless CC License in place (see abstract).